Oil & Natural Gas Technology

DOE Award No.: DE-FC26-06NT43067

Quarterly Progress Report
(April - June 2009)

Mechanisms Leading to Co-Existence of Gas and Hydrate in Ocean Sediments

Submitted by:
The University of Texas at Austin
1 University Station C0300
Austin, TX 78712-0228

Prepared for:
United States Department of Energy
National Energy Technology Laboratory

July 29, 2009

Office of Fossil Energy

MECHANISMS LEADING TO CO-EXISTENCE OF GAS AND HYDRATE IN OCEAN SEDIMENTS

CONTRACT NO. DE-FC26-06NT43067

QUARTERLY PROGRESS REPORT
Reporting Period: 1 Apr 09 – 30 Jun 09

Prepared by

Steven L. Bryant
Department of Petroleum and Geosystems Engineering
The University of Texas at Austin
1 University Station C0300
Austin, TX 78712-0228
Phone: (512) 471 3250
Email: steven_bryant@mail.utexas.edu

Ruben Juanes
Department of Civil and Environmental Engineering
Massachusetts Institute of Technology
77 Massachusetts Avenue, Room 48-319
Cambridge, MA 02139
Phone: (617)253-7191
Email: juanes@mit.edu

Prepared for
U.S. Department of Energy - NETL
3610 Collins Ferry Road
P.O. Box 880
Morgantown, WV 26508

Summary

One the key activities during this reporting period has been the extension of the coupled code of two-phase flow and sediment mechanics, in the framework of PFC3D. While much of the dynamics between fluid displacement and grain movement could be understood with 2D representations, we need to extend the model from 2D to fully 3D in order to account for hydrate formation, which is the objective of Task 7 of this project. Here, we report on such extension. We have made several improvements in terms of the physics formulation, as well as on the communication between the mechanics and flow codes. Improvement is still needed in some areas (such as incorporating dynamics in the pore-scale fluid displacement), and we address those in this report as well. Current work, not reported here, is focused on incorporating hydrate formation.

During this reporting period, a peer-reviewed paper was accepted for publication in Journal of Geophysical Research. The paper is a synthesis of the MS thesis by Antone Jain, which was completed in May 2009 and is submitted along with this progress report. Two talks were given at the US National Congress on Computational Mechanics, held in Columbus, OH, in July 2009. We have updated the publication list on the NETL project database.

Activities in This Reporting Period

Task 7.0 - Coupled gas/water/sediment dynamics with hydrate formation

We have developed a three-dimensional (3D) grain-scale model of a deformable porous medium, coupling sediment mechanics with two-phase flow. The model has been used to simulate drainage of a marine sediment by invasion of methane gas, while accounting for the mechanical deformation associated with the presence of the fluids. We track the gas-water interface at the pore level, and compute the repulsive pressure forces acting on the grain surfaces and the cohesive forces provided by the water menisci. The simulations capture the crossover between ordinary capillary invasion in which the sediment matrix behaves essentially as rigid and mechanically-assisted invasion or "capillary fracturing" where the sediment deformation provides a preferential pathway for the gas migration.
In our model, a sediment sample is represented by 3D, disordered packing of spherical grains. The void space is mapped into a pore network through Delaunay tessellation: each pore body is the void inside a tetrahedral volume defined by the nearest four grain centers, and is connected to exactly four neighbors through triangular faces. To simulate the mechanical deformation of the solid skeleton we use the Discrete Element Method (DEM). Scaling analysis reveals that for a wide range of sediment and fluid properties, the time scale associated with the drainage of a single pore is much smaller than that which is required for the solid skeleton to relax into a static mechanical equilibrium. Based on this argument we adopt the quasi-static Invasion-Percolation (IP) model for fluid/fluid displacement.

The DEM code PFC3D [ITASCA, 2008] serves as the computational platform from which we execute our fluid-related modules. These modules are coded in Matlab [The MathWorks Inc., 2009], modifying the quasi-static, finite-network drainage simulation code by Behseresht [2008] and adding modules to compute the fluid-related forces. To avoid the slow process of file exchange between different software, we compiled the Matlab codes into C++ shared libraries using the Matlab Compiler toolbox [The MathWorks Inc., 2009], which are then compiled together with PFC3D source codes to create a single private executable. In addition to the DEM computational cycle, two types of user-defined modules are called from within this executable: (a) initialization, pre- and post-processing, invoked prior and after the simulation of drainage; and (b) update of gas-water interface location and fluid-related forces, called at each time step in the simulation from within the DEM cycle, prior to the integration of the equation of motion performed to obtain the grain displacements and rotations.

Noting that in many geological systems the time scale associated with variations in gas pressure P_g (and the corresponding capillary pressure, $P_c=P_g-P_w$, where P_w is the water pressure) is much larger than that associated with relaxation of the solid-fluid system into a new equilibrium configuration, we consider the following scenario: following a pressure increment, ΔP_c, the sediment achieves steady-state before another increment is applied. Further simplification is achieved by invoking the aforementioned scaling argument regarding the fast relaxation of the fluids, staggering the update of the flow and grain displacements: at a given IP step, we first advance the gas-water interface neglecting the effect of the deformations, and then compute the associated matrix deformations. Finally, to prevent masking of the coupling with mechanics by the large avalanches typical of disordered systems, we restrict the number of pores invaded at a given IP step. The computational cycle is presented in Figure 1. Efficient numerical implementation enables us to simulate drainage using packs made of tens of thousands of grains/pores, and to capture the complex patterns of the fluid configuration and intergranular force distribution.

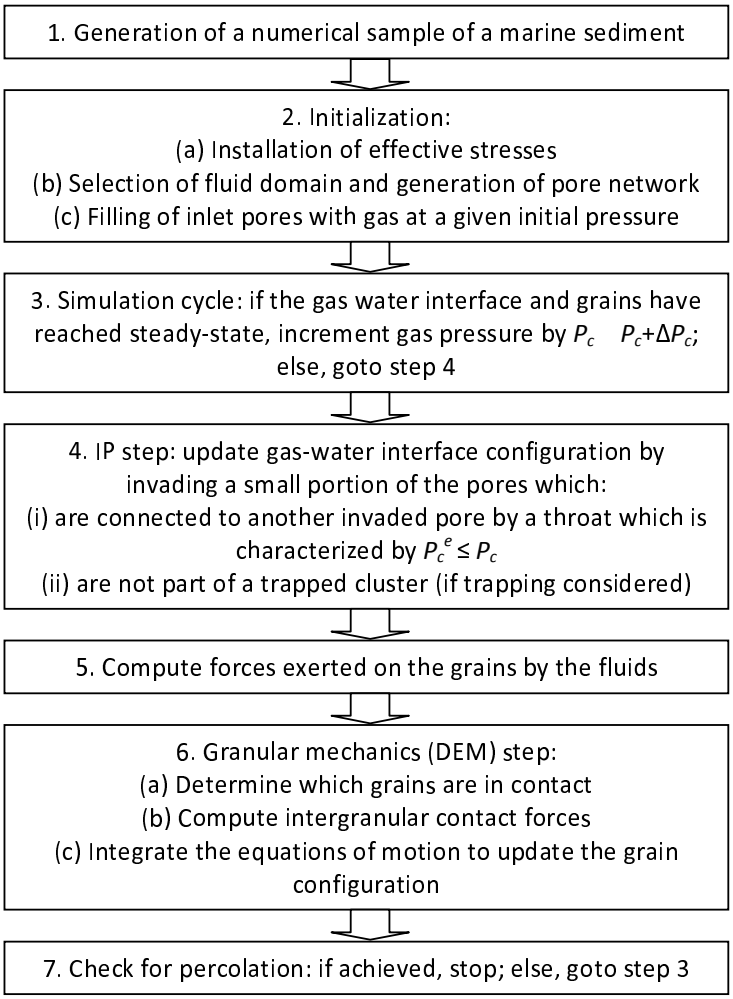

Figure 1 – Computational cycle used in the simulations. See text below for further details and notations.

Three types of sediments are considered here: (a) unconsolidated, i.e. a granular material; (b) consolidated, where the grains are cemented at their contacts; and (c) fractured. The intergranular contact loads consist of normal compressive forces, shear forces, and moments, evaluated using Hertz-Mindlin constitutive relations. In the unconsolidated sediment the only source of cohesion is the meniscus pinning, which we compute *via* the numerical approximation of the Young-Laplace equation in Willett et al. [2000]. In cemented sediments, (b)-(c), additional tensile forces due to cement at the contacts are modeled by the "parallel-bond" model [Potyondy and Cundall, 2004].

In IP, a pore can be drained if it is connected to another invaded pore by a throat with a capillary entry pressure, P_c^e, which is lower or equal to the current capillary pressure, P_c. We estimate P_c^e according to the Mason and Mellor [1995] correction for Haines [1930] model. Our model includes evaluation of the stability of pendular rings/liquid bridges, and the meniscus volume, estimated assuming toroidal shape. The model accounts for trapping of the wetting phase, considering connectivity either through the pore throats

alone or the liquid bridges as well. Trapping can be neglected if the timescales of interest are long enough to consider flow along water films coating the grains.

Following the generation of the numerical sample, namely a grain pack and a corresponding pore network, we apply the following initial and boundary conditions. For the solid skeleton we prescribe the macroscopic effective stress, which represents *in-situ* earth stresses. The macroscopic stresses, measured by the forces applied on planar elastic walls which enclose the pack, are enforced through the wall displacements. For the flow, initial conditions are set by assigning several pores on the lower ($-z$) face as inlets, installing in them gas with a given initial pressure. The pores on the opposite face ($+z$) are defined as the outlet, which, if invaded, mark percolation and the end of the simulations. Other pores along the outer faces serve as no-flow boundaries.

Boundary effects can arise due to the solid-fluid coupling: invasion may alter the stress state, whereas tessellation near the planar boundaries leads to distorted pore shapes. To alleviate these undesired effects, we separate the solid and fluid domains by defining an inner portion of the granular pack as a "fluid region", *cf.* Figure 2. The resulting region provides a well-defined, physically representative network of pores in which drainage is simulated. Granular mechanics is simulated within the entire pack.

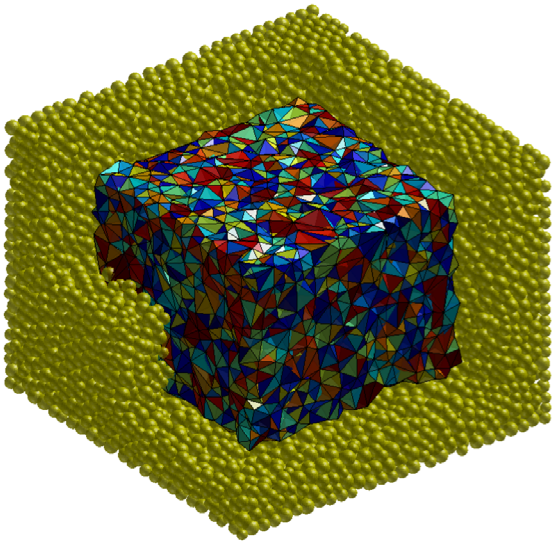

Figure 2 – An internal part of the grain pack is selected as a "fluid" domain in which flow is simulated, while intergranular interactions are computed within the entire pack. Placing the boundaries of the solid and fluid domains far apart alleviates the boundary effects associated with coupling of flow and deformation.

Results of the simulations show that in fine-grained sediments, the large capillary pressures required for drainage exert forces on the grains which are comparable to the intergranular contact forces. Consequently, the sample deforms, in particular in regions adjacent to the gas-water interface, and the coupling between flow and mechanics becomes notable: the percolation pressure is significantly lower than that predicted assuming a perfectly-rigid matrix, and the invasion pattern is often focused in a small region. In addition, the percolation threshold is reached by an avalanche-like event, where invasion proceeds with no further increase of P_c, see Figure 3. Conversely, the lower capillary pressures at percolation in coarser samples are similar to those expected for a rigid matrix, often with a more ramified invasion pattern than in fine-grained samples, and less sharp percolation threshold which follows several avalanches. These avalanches are caused by the throat distribution along the percolating cluster alone, and are not affected by the mechanics. These results extend the two-dimensional (2D) analysis by Jain & Juanes [2009] and Jain [2009].

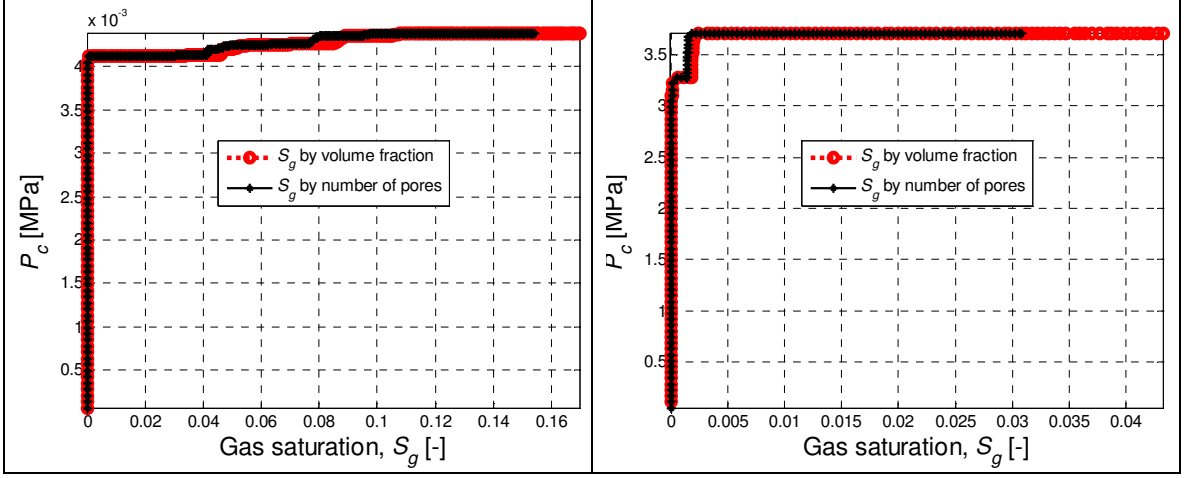

Figure 3 – Gas saturations *vs*. capillary pressure, for the coarse- (left) and fine-grained (right) consolidated samples, with mean grain size of 100 and 0.12 μm, respectively. Percolation in the finer sample is reached through a single avalanche-like event, which proceeds by displacing grains and breaking cement, with no further increase of the pressure. The invasion into the coarser sample is more gradual.

To illustrate the above, in Figures 4-5 we plot the pores invaded at percolation. In all samples the grain size is uniformly distributed by 0.25 around the mean. Figure 4 shows the different invasion patterns in a coarse- and fine-grained consolidated numerical samples. In Figure 5 we plot the results obtained for a fractured sediment. We simulate the effect of a preexisting *closed* fracture along x=0 by removing the cement bonds within a thin layer around that plane. Thus, the fracture aperture is initially zero. While such removal does not perturb the initial throat distribution, it will affect its evolution through the localized deformations. Figure 5 also demonstrates that percolation pressure reduces with the stress. This behavior is caused by further opening of the fracture under lower confinement, allowing a larger portion of the fractured region to be invaded.

We note that the gas volumetric saturation may not be indicative of the crossover between the two types of invasion, since it is affected by two competing processes: in finer sediments gas tends to invade a smaller percentage of the pores, whereas the volume of these pores tends to increase due to the high pressures, thus increasing the volume-fraction based saturation.

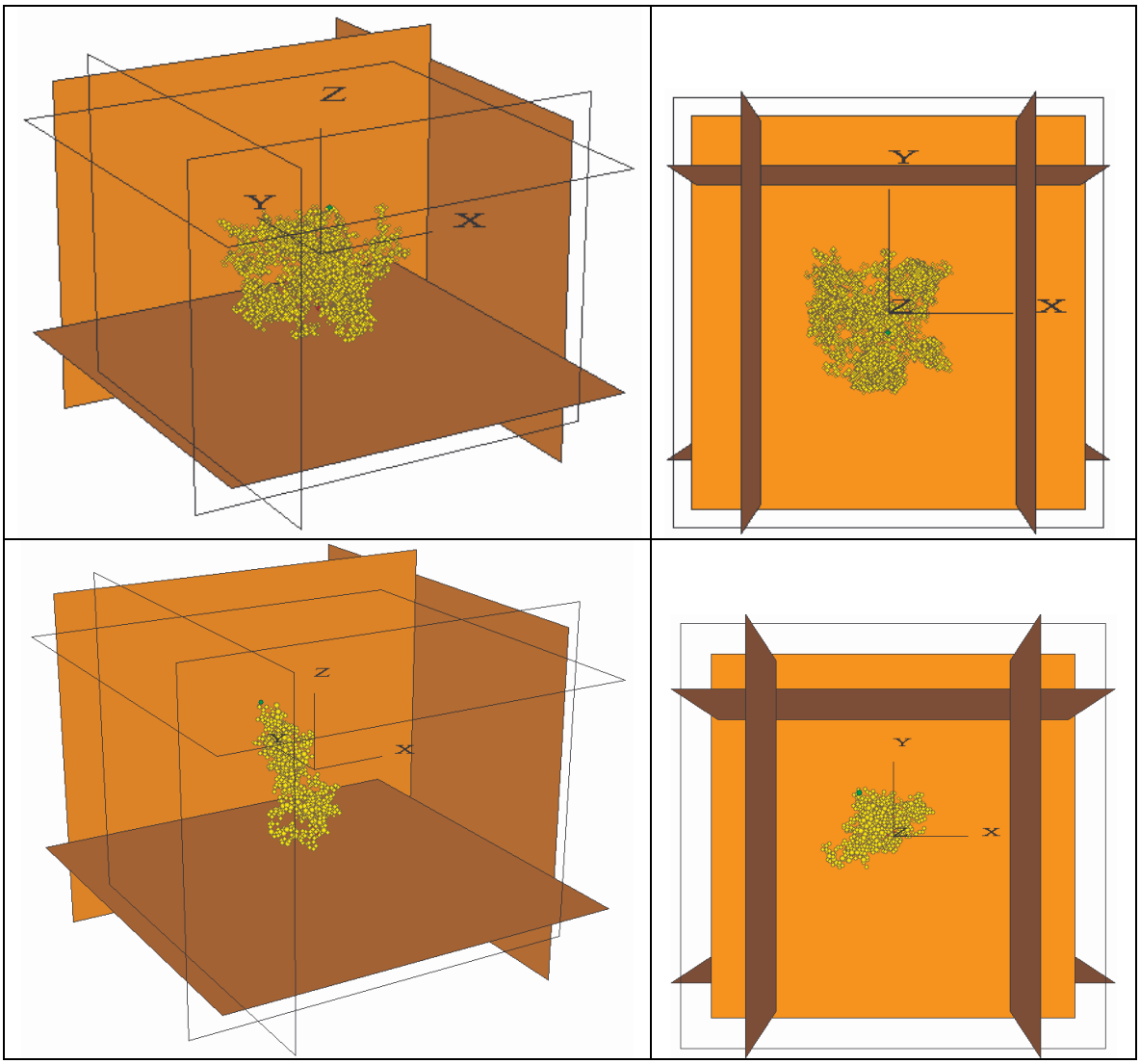

Figure 4 – Simulating percolation in consolidated sediments. For each sample, two views of the pores invaded are shown, plotting each pore as a sphere with a volume equivalent to that computed by tessellation. Top: a sample with a mean grain size of 100 μm. The capillary pressure, P_c, is 4.4KPa and the gas saturation, S_g, is 17%. Bottom: a fine-grained sample with a mean grain size of 0.12 μm, with P_c=3.5MPa and S_g=4%. Anisotropic effective stresses of $\sigma_z=\sigma_y=2\sigma_x$=0.48MPa have been applied.

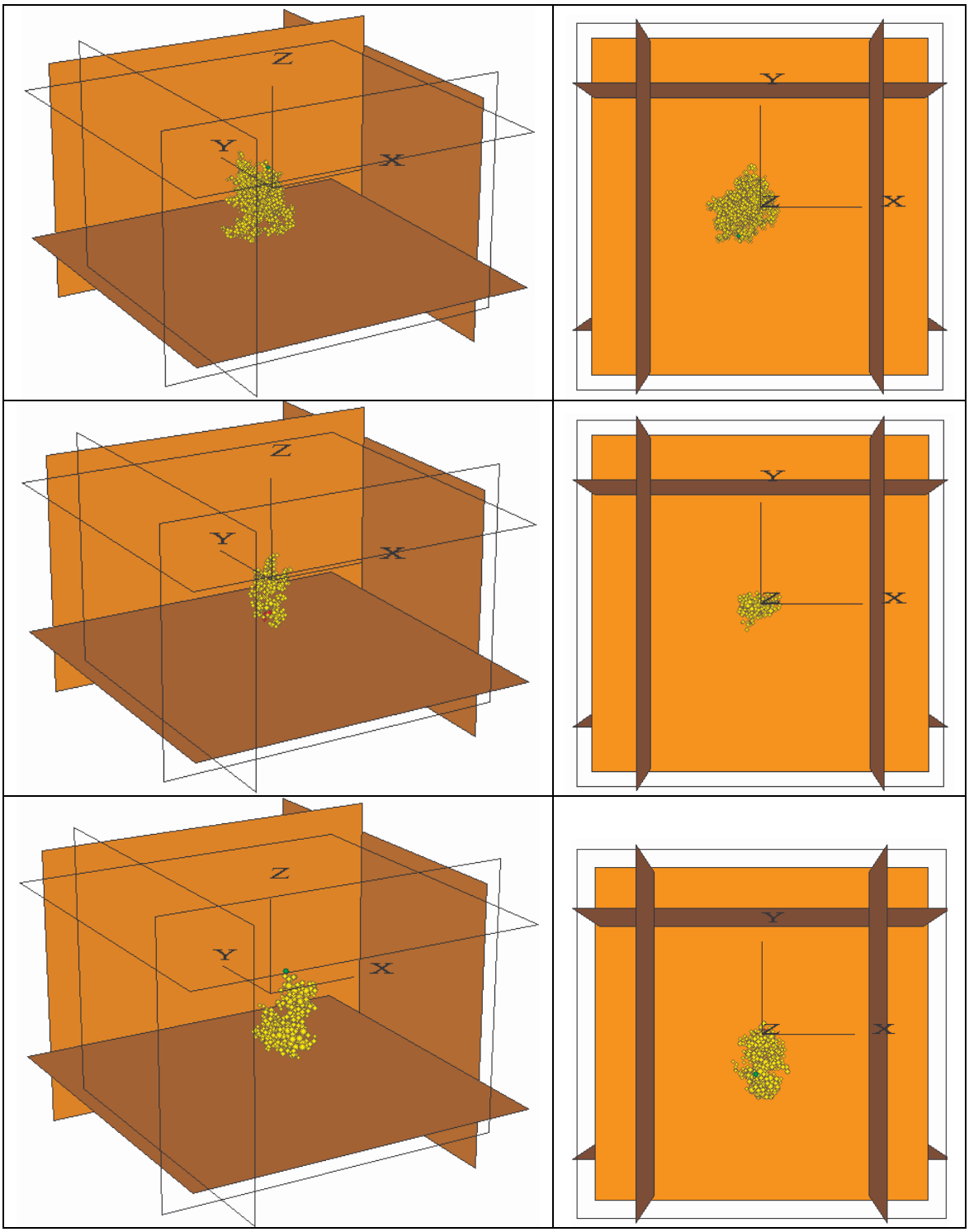

Figure 5 – Simulating percolation in sediments fractured along x=0. For each sample, two views of the pores invaded are shown, plotting pores as spheres with volumes equivalent to those computed by tessellation. Top: a sample with a mean grain size of 50 μm, with P_c=9.4KPa and S_g=8%. Center: a fine-grained sample with a mean grain size of 0.05 μm, with P_c=6.5MPa and S_g=3%. Anisotropic effective stresses of σ_z=1.25σ_y=2σ_x=1MPa have been applied on the top and middle samples. Bottom: reducing the stresses applied on the fine-grained sample to σ_z=σ_y=2σ_x=0.48MPa lowered the percolation pressure to P_c=5.7MPa, with S_g=6%.

To highlight the crossover between ordinary capillary invasion in coarse-grained sediments and "capillary fracturing" in fine-grained sediments, in Figure 6 we plot the percolation pressure *vs*. the mean grain size. The linear fit of the data for the coarser samples corresponds to a line with a slope of approximately –1, which is due to the dependence of P_c^e on the inverse of grain size, R, with no mechanical coupling. The pressures observed for the finer samples lie beneath this line, demonstrating that coupling with mechanical deformation assists the invasion. The reduction in coupling strength with grain size is evident from the results of simulations assuming a rigid matrix, which, for samples with grains larger than 1μm are practically identical to the results obtained with the coupled model. For the given sediment and fluid properties used in those simulations, the crossover between ordinary capillary invasion and mechanically-assisted invasion occurs at grain sizes smaller than ~0.1μm, in accordance with the values reported by Jain & Juanes [2009].

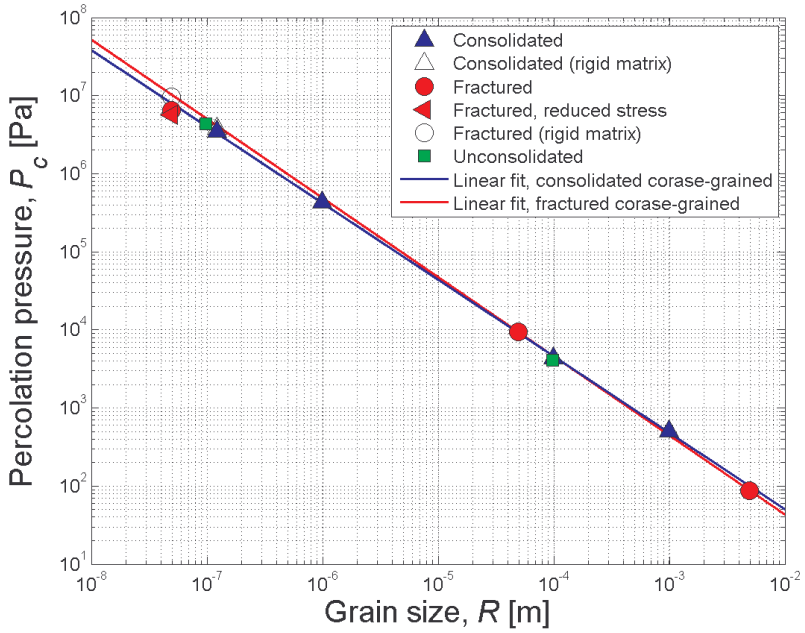

Figure 6 – Percolation pressure *vs*. mean grain size for consolidated, fractured and uncemented sediment samples. Also plotted are the linear fit of the data for the coarser samples (consolidated and fractured), with a slope of ~ –1 due to the $1/R$ dependence of P_c^e lacking mechanical coupling. The fact that the pressures in the finer samples lie beneath this line together with the higher pressures observed in simulations assuming rigid matrix, demonstrate the coupling with mechanical deformation.

We analyze these results *via* a dimensionless "coupling strength" parameter, N_{cf}, defined as the ratio of the characteristic pressure force and the force required to sufficiently displace the grains so that the percolation pressure is altered. If N_{cf}>>1, coupling with mechanics dominates and the percolation pressure will be significantly lower than that anticipated with no matrix deformation. In general, N_{cf} depends on the *initial* packing and network properties, e.g. throat distribution, as well as the sensitivity of these properties to grain displacements which controls their *evolution* with the invasion. Particularly, N_{cf} scales with inverse of the grain size, the interfacial tension, and the inverse of the intergranular stiffness and the effective stress. It also scales with the inverse of a

characteristic intergranular strain, ε_{cf}. This strain is a function of both the throat distribution along the percolating path as well as the degree of inelasticity, e.g. tendency of the system towards rearrangements *vs*. elastic intergranular deformations. Thus, the value of ε_{cf} emanates from the pack's microstructure. A quantitative analysis of the packing disorder using statistical tools, which requires very large systems and possibly simpler microscopic models, is underway.

The preliminary results described above have important implications on the hydrate distribution within marine sediments. Experimental observations indicate that: (a) coarse-grained sediments are associated with higher hydrate saturations [Ginsburg et al., 2000; Torres et al., 2008]; and (b) at deeper formations, hydrates tend to form more vertical patterns, in a vein- or fracture-filling manner, whereas sediments at shallower depths are characterized by smaller dip angles of hydrate layers with more cross-cutting of the original strata, and highly variable saturations [Abegg et al., 2007]. These observations are typically explained by the capillary inhibition and segregation mechanisms for the hydrate growth [Clennell et al., 1999]. Focusing on methane migration rather than on hydrate growth mechanisms, we offer a different explanation: reduction in grain size and stress (depth) strengthen the invasion-mechanics coupling, causing greater disturbance to the original sediment matrix, with capillary-fractures that are dictated by the distribution of the throat sizes as well as the grain microstructure and their mechanical properties. If all methane is converted to hydrate, hydrate will tend to cross-cut the sediment layers with random fracture orientation and spatially variable saturation. In deeper sediments, the large stresses inhibit the deformation, and may force methane to migrate by opening of preexisting fractures. If such fractures were caused by in-situ stresses, their slopes, and consequently the slopes of hydrate veins, will tend to be steep. Another important aspect of our results is in estimating the amounts of methane that can reach the water column. Previous studies often assume that hydrate formation in fine-grained sediments forms a barrier to methane transport (e.g. see Kleinberg et al. [2003] and the references therein). According to our model, in active regions characterized by high gas fluxes methane can flow rapidly through coarse-grained sediments by ordinary percolation, while traversing through fine-grained sediments by the proposed capillary-fracturing mechanism. In such cases, hydrate formation may be inhibited because of local water depletion, hypersalinity, or capillary inhibition [Clennell et al., 1999], and the amounts of methane that can traverse the hydrate stability zone will be large.

To summarize, the model presented here captures the crucial coupling between multiphase flow and mechanics, and provides an estimate of the range of sediment and fluid properties in which coupling dominates drainage. A series of scaling arguments together with efficient numerical implementation allows us to use packs of order 10^4 grains in the simulations, which is required to describe the complex interactions between the solid grains and fluids in 3D. We note, however, that this model is valid only under restrictive underlying assumptions, and may need to be modified in order to evaluate the sediment response under different conditions. In particular, staggering of the update for the flow and mechanics (see Figure 1), the use of a quasi-static IP model and the restriction of the number of pores invaded at each IP step may lead to erroneous results when simulating drainage in sediments made of extremely small and soft grains under low effective stress. It is not clear if those regimes must be considered to capture the transition between ordinary invasion and capillary fracturing in real marine sediments.

Furthermore, under such extreme conditions the numerical simulations often become unstable, and the mechanical equilibrium of the solid grains following the invasion may not be physically representative. To overcome these difficulties we plan to introduce dynamics into the flow model in the form of pressure propagation upon invasion. Such model, by representing the finite time it takes for the gas-water interface to advance within the pore throats, will also regularize the numerical algorithm, making it more stable.

Our current efforts focus on introducing hydrate growth and dissociation into our sediment model, and quantifying the impact of hydrates on the mechanical and flow properties of a hydrate-bearing sediment. We consider a scenario in which the capillary pressure variations occur over much longer timescales than those associated with methane hydrate formation and growth, thus modeling hydrate growth along a *static* interface which location is *known* from the coupled flow-mechanics described above. The growth kinetics including inhibition due to hypersalinity will be evaluated using mass balance analysis for methane, water and salt in all pores along the interface, as well as published data from grain-scale experiments, e.g. [Freer et al., 2001; Taylor et al., 2007].

Task 8.0 - Modeling methane transport at the bed scale

We have started the development of a mathematical model of methane migration and hydrate formation/dissociation at the bed scale, which will incorporate the two main mechanisms of methane gas invasion: capillary invasion and sediment fracturing.

- At this scale, the pressure at the rising methane/water interface depends on rate of hydrate formation, the height of the connected methane volume and, for fractures, the rate of drainage into porous beds. We will explore whether this coupling leads to self-reinforcing or self-limiting transport, and whether this helps or hinders subsequent transport events in the same sediment volume.
- We will develop a quasi-1D model for methane transport at the bed scale. The model will determine whether vertical migration of gas through the HSZ (either by fracture opening or capillary invasion) and lateral movement along beds are possible. The key variable governing the process is the capillary pressure P_c, which depends on the height of the connected gas zone below the HSZ.
- The model will account for leakage due to lateral migration into sediment beds, and leakage rates will be evaluated using a mass transfer coefficient approach.
- The appropriate expressions of the mass transfer coefficient that reflect the outcome of the modeling at the pore scale will be determined from previous tasks.
- The ultimate distribution of hydrate within the HSZ will be obtained for the different scenarios: (1) assuming that methane migrates through sediment that is initially depleted in hydrate; (2) assuming that hydrate forms readily at the gas-water interface; and (3) assuming that hydrate forms only when upwards movement of methane gas stops, either by an increase in resistance to flow or by loss of pressure in the gas phase.

Bibliography

Abegg, F., Bohrmann, G., Freitag, J., and Kuhs, W. (2007). Fabric of gas hydrate in sediments from Hydrate Ridge - results from ODP Leg 204 samples. Geo-Marine Letters, 27(2):269–277.

Behseresht, J. (2008). Infinite-Acting Physically Representative Networks for Capillarity-Controlled Displacements, MS thesis, The University of Texas, Austin, TX.

Clennell, M. B., Hovland, M., Booth, J. S., Henry, P., and Winters, W. J. (1999). Formation of natural gas hydrates in marine sediments: 1. Conceptual model of gas hydrate growth conditioned by host sediment properties. Journal of Geophysical Research, 104(B10):22985–23003.

Freer, E. M., Selim, M. S. and Sloan, E. D. (2001). Methane hydrate film growth kinetics. Fluid Phase Equilibria, 185:65–75.

Ginsburg, G., V. Soloviev, T. Matveeva, and Andreeva, I. (2000). Sediment grain size control on gas hydrate presence, sites 994, 995, and 997, Proc. Ocean Drilling Program Scientific Results, 164:237– 245.

Haines, W. B. (1930). Studies in the Physical Properties of Soil. V. The hysteresis effect in capillary properties and the modes of moisture distribution associated therewith. Journal of Agricultural Sciences 20:97.

ITASCA (2008). PFC3D v4.0, Itasca Consulting Group, Inc., Minneapolis, MN.

Jain, A. K. (2009). Preferential Mode of Gas Invasion in Sediments: Grain-Scale Model of Coupled Multiphase Fluid Flow and Sediment Mechanics, MS thesis, Massachusetts Institute of Technology, Cambridge, MA.

Jain, A. K., and Juanes, R. (2009). Preferential mode of gas invasion in sediments: Grain-scale mechanistic model of coupled multiphase fluid flow and sediment mechanics, Journal of Geophysical Research, (in press).

Kleinberg, R. L., Flaum, C., Griffin, D. D., Brewer, P. G., Malby, G. E., Pelzer, E. T., and Yesinowski, J. P. (2003). Deep sea NMR: methane hydrate growth habit in porous media and its relationship to hydraulic permeability, deposit accumulation, and submarine slope stability. Journal of Geophysical Research, 108(B10):2508.

Mason, G. and Mellor, D. W. (1995). Simulation of Drainage and Imbibition in a Random Packing of Equal Spheres. Journal of Colloid and Interface Science 176:214-225.

Taylor, C. J., Miller, K. T., Koh, C. A. and Sloan, E. D. (2007). Macroscopic investigation of hydrate film growth at the hydrocarbon/water interface. Chemical Engineering Science, 62(23):6524-6533.

The MathWorks Inc. (2009). MATLAB, The Language of Technical Computing, Version 7.8.0.347 (R2009a).

Torres, M. E., Trehu, A. M., Cespedes, N., Kastner, M., Wortmann, U. G., Kim, J.-H., Long, P. E., Malinverno, A., Pohlman, J. W., Riedel, M., and Collett, T. S. (2008). Methane hydrate formation in turbidite sediments of northern Cascadia, IODP Expedition 311, Earth Planetary Science Letters, 271:170– 180.

Willett, C. D., Adams, M. J., Johnson S. A. and Seville J. P. K. (2000). Capillary bridges between two spherical bodies. Langmuir 16:9396–9405.

National Energy Technology Laboratory

626 Cochrans Mill Road
P.O. Box 10940
Pittsburgh, PA 15236-0940

3610 Collins Ferry Road
P.O. Box 880
Morgantown, WV 26507-0880

One West Third Street, Suite 1400
Tulsa, OK 74103-3519

1450 Queen Avenue SW
Albany, OR 97321-2198

2175 University Ave. South
Suite 201
Fairbanks, AK 99709

Visit the NETL website at:
www.netl.doe.gov

Customer Service:
1-800-553-7681